



**Australian Government**  
**Bureau of Meteorology**

**The Centre for Australian Weather and Climate Research**  
A partnership between CSIRO and the Bureau of Meteorology



# Sedimentation of volcanic ash in the HYSPLIT dispersion model

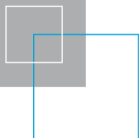
Richard A. Dare

**CAWCR Technical Report No. 079**

**January 2015**



[www.cawcr.gov.au](http://www.cawcr.gov.au)





# Sedimentation of volcanic ash in the HYSPLIT dispersion model

Richard A. Dare

*Centre for Australian Weather and Climate Research, Australian Bureau of Meteorology*

**CAWCR Technical Report No. 79**

January 2015

National Library of Australia Cataloguing-in-Publication Entry:

ISSN: 1836-019X

Author: Richard A. Dare

Title: Sedimentation of volcanic ash in the HYSPLIT dispersion model

ISBN: 978-1-4863-0495-0

Series: CAWCR Technical Report; No. 079.

Notes: Includes bibliographical references and index.

Subjects: Volcanic ash, tuff, etc.

Aeronautics--Safety measures.

Aircraft accidents--Prevention.

Dewey Number: 629.1324

Enquiries should be addressed to:  
Richard A. Dare  
Centre for Australian Weather and Climate Research:  
Australian Bureau of Meteorology  
GPO Box 1289, Melbourne  
Victoria 3001, Australia

r.dare@bom.gov.au

## Copyright and Disclaimer

© 2010 CSIRO and the Bureau of Meteorology. To the extent permitted by law, all rights are reserved and no part of this publication covered by copyright may be reproduced or copied in any form or by any means except with the written permission of CSIRO and the Bureau of Meteorology.

CSIRO and the Bureau of Meteorology advise that the information contained in this publication comprises general statements based on scientific research. The reader is advised and needs to be aware that such information may be incomplete or unable to be used in any specific situation. No reliance or actions must therefore be made on that information without seeking prior expert professional, scientific and technical advice. To the extent permitted by law, CSIRO and the Bureau of Meteorology (including each of its employees and consultants) excludes all liability to any person for any consequences, including but not limited to all losses, damages, costs, expenses and any other compensation, arising directly or indirectly from using this publication (in part or in whole) and any information or material contained in it.

All images reproduced in grayscale. A colour version of CAWCR Technical Report No.079 is available online: <http://www.cawcr.gov.au>

# Contents

<b>Executive Summary .....</b>	<b>1</b>
<b>1 Introduction .....</b>	<b>2</b>
<b>2 Terminal fall velocity formulation .....</b>	<b>3</b>
<b>3 Properties of volcanic ash particles .....</b>	<b>5</b>
3.1 Density .....	5
3.2 Shape.....	5
3.3 Size .....	6
<b>4 Model simulation results: gas versus solid particles.....</b>	<b>7</b>
4.1 Introduction .....	7
4.2 18-hour model forecast of volcanic ash dispersion .....	7
4.3 24-hour model forecast of volcanic ash dispersion .....	10
4.4 Domain-integrated mass of volcanic ash.....	11
<b>5 Model results: physical properties of particles .....</b>	<b>15</b>
5.1 Introduction .....	15
5.2 Mass remaining in atmosphere.....	15
5.3 Surface deposition of volcanic ash .....	18
5.4 Volcanic ash concentration in the10000-15000 metre layer .....	19
<b>6 Summary.....</b>	<b>21</b>
<b>7 Recommendations .....</b>	<b>24</b>
<b>8 References.....</b>	<b>25</b>

## List of Figures

Fig. 1	Differences in TFV predicted by the Stokes and Ganser equations versus particle diameter. ....	4
Fig. 2	Particle size distribution (particle diameter versus percentage of mass contained in each discrete particle size bin). With a peak percentage centred on 20 micron, this PSD is referred to as PSD-20. ....	6
Fig. 3	Mean layer (0-5000 metres) concentration of volcanic cloud at 02 UTC 31 May 2014, 18 hours after the eruption began, for (a) gas simulation, (b) solid particle simulation. The location of the source volcano is shown by the black dot, and the location of Darwin is shown by "D". ....	9
Fig. 4	Mean layer (5000-10000 metres) concentration of volcanic cloud at 02 UTC 31 May 2014, 18 hours after the eruption began, for (a) gas simulation, (b) solid particle simulation. The location of the source volcano is shown by the black dot, and the location of Darwin is shown by "D". ....	10
Fig. 5	Mean layer (0-5000 metres) concentration of volcanic cloud at 08 UTC 31 May 2014, 24 hours after the eruption began, for (a) gas simulation, (b) solid particle simulation. The location of the source volcano is shown by the black dot, and the location of Darwin is shown by "D". ....	12
Fig. 6	Mean layer (5000-10000 metres) concentration of volcanic cloud at 08 UTC 31 May 2014, for (a) gas simulation, (b) solid particle simulation. ....	13
Fig. 7	Mass versus height display of layer- and areal-integrated mass load of solid particles during the 24 hour period following the end of the eruption, for the three layers 0-5000, 5000-10000 and 10000-15000 metres. ....	14
Fig. 8	Particle size distributions (particle diameter versus percentage of mass contained in each discrete particle size bin), with a peak percentage centred on (a) 6.5 micron (PSD-6.5) and (b) 65 micron (PSD-65). Dashed lines represent the original PSD shown by Fig. 2. ....	17
Fig. 9	Mass remaining in the atmosphere (percentage of total mass released) after a simulated period of 24 hours, for each of the thirteen experiments listed in Table 1... ..	18
Fig. 10	Time-integrated (based on 1-hourly model output) surface deposition of volcanic ash (solid particles) over a 40-hour period since the beginning of the eruption. The location of the source volcano is shown by the black dot, and the location of Darwin is shown by "D". ....	20
Fig. 11	Mean layer (10000-15000 metres) concentration of volcanic ash cloud at 08 UTC on 31 May 2014, 24 hours after the eruption began for experiments 2, 11, 12, 13, and 1. ....	20

## List of Tables

Table 1	Physical properties of volcanic ash particles used in each model experiment. ....	6
---------	---	---

## EXECUTIVE SUMMARY

Solid ash particles injected into the atmosphere during volcanic eruptions have the potential to cause significant damage to aircraft engines, endangering lives and requiring expensive repairs. The aviation industry also suffers financially when flight operations are disrupted due to the presence of volcanic ash clouds in the vicinity of airports and flight paths. For all of these reasons it is important to improve the accuracy of observations and predictions of volcanic ash clouds.

Forecasters in the Australian Bureau of Meteorology's Volcanic Ash Advisory Centre (VAAC) rely on a variety of observations and numerical model guidance. In this report, aspects of the numerical modelling are addressed. Solid ash particles were introduced to the model to replace the use of volcanic gas in the model forecasts. To ensure accurate prediction of the terminal fall velocity of volcanic ash particles, the Stokes equation was replaced with the Ganser formulation. Appropriate values of density, shape and size were adopted to represent the properties of volcanic ash particles. A total of thirteen model experiments were conducted, the first simulating dispersion of a gas and the second the dispersion of solid particles. The experiment using solid particles simulated movements of volcanic ash particles with a level of physical realism not achieved by the gas-based experiment. The introduction of solid volcanic ash particles impacted upon volcanic ash cloud concentrations, areal extent of volcanic ash clouds, and the total mass of volcanic ash removed from the model atmosphere over time. The eleven model experiments that followed the first two assessed the sensitivity of the model results to changes in the physical properties of the solid particles and the choice of the particle size distribution.

Following from the findings in this report, these recommendations are made:

- It is recommended that the Ganser terminal fall velocity equation be implemented in the operational version of the HYSPLIT model, as it is more appropriate for the prediction of terminal fall velocities of volcanic ash particles than the Stokes equation.
- It is recommended that the more physically realistic model configuration with a particle size distribution and improved particle fall speed should replace the current dispersion model runs that assume a gas.
- It is recommended that the model configuration established in this report be used as the basis for the development of an ensemble system for the prediction of volcanic ash cloud dispersion.
- In future, other processes in the dispersion model that affect the fallout of solid volcanic ash particles should be reviewed and considered carefully, such as wet deposition, aggregation, convective motions, and the representation of turbulent mixing, as they all have the potential to impact the predicted concentrations and areal extents of volcanic clouds.
- It may be beneficial in future to review and test the choice of model level heights to find a set of levels that best represents the needs of forecasters when relying on numerical model guidance of volcanic ash at specific flight levels.
- Numerical model guidance accuracy may benefit in future from the possible coupling of a dispersion model with an eruption column plume model. In the past, these different types of models have been operated independently. Problems and impacts of coupling these different types of systems are unknown, but are likely to be quite complicated, and would need to be planned and investigated carefully.

# 1 INTRODUCTION

The Hybrid Single-Particle Lagrangian Integrated Trajectory (HYSPLIT) model (Draxler and Hess 1997) is used by the Australian Bureau of Meteorology's Volcanic Ash Advisory Centre (VAAC) to assist in the prediction of the movement of volcanic ash clouds. In the past, the VAAC has operated this model using a gas to represent the cloud produced from an eruption because physical properties of ash particles were not well known. Although gases are produced by volcanic eruptions in addition to solid ash particles, it is the ash which is of primary interest due to its potential to damage aircraft engines.

In the atmosphere, gases and solid particles behave differently from each other. A gas that is released from a volcano will be transported along with other gases present in the atmosphere. Solid particles will be subject to the same atmospheric motions, but in addition, solid particles will descend towards the ground due to the Earth's gravity. The largest solid particles fall to the ground first, near the volcano, while smaller particles that take a longer time to fall will disperse over a wider area due to movement by winds and turbulence. In addition to size, other properties of a particle will also influence the speed at which it falls. A particle of higher density will descend faster, and a particle shape that is closer to that of a sphere will generally fall with a higher speed. Atmospheric properties will also influence the speed of descent. Putting aside vertical motions of air within the atmosphere, the terminal fall velocity (TFV) of a particle will be smaller at lower elevations due to the larger air density closer to the Earth's surface.

An aim of this project is to alter the use of the model so that simulations involve the dispersion of solid particles rather than gas. This change is made to improve the realism of the physical system being modelled, with the aim of improving the accuracy of the model's predictions. This may be achieved by considering two points. First, the model's formulations may be modified to more closely represent the true nature of the atmosphere and, in this case, the behaviour of particles within the atmosphere. Second, numerical data used to represent physical entities within the model may be improved by applying more realistic values.

Implementing the change from gas to solid particles involves a number of steps. The first is to assess the suitability of the model for simulating volcanic ash clouds containing solid particles. It is already well known that the HYSPLIT model has the ability to predict the movement of both gases and particles, and that it includes the influence of gravity on solid particles (Draxler and Hess 1997). Therefore, this initial step involves an assessment of the ability of the particular formulation within the model to accurately predict the gravitational descent of solid particles (Section 2). The second step is to define a set of properties that describes volcanic ash particles (density, shape and size), discussed in Section 3. The results from modelling the dispersion of gas compared with the dispersion of solid particles are discussed in Section 4. The sensitivity of the simulations to the physical properties of particles are considered in Section 5, followed by conclusions in Section 6.

## 2 TERMINAL FALL VELOCITY FORMULATION

The HYSPLIT model has for many years included a formulation to predict the TFV of solid particles (Draxler and Hess, 1997). The formulation is the well-known Stokes equation, as shown by Equation 1.

$$TFV = \frac{(\rho_p - \rho_{AIR})g d^2}{18 \mu K} \quad (1)$$

where  $\rho_p$  is the density of the particle,  $\rho_{AIR}$  is air density,  $g$  is gravitational acceleration,  $d$  is the particle diameter,  $\mu$  is dynamic viscosity and  $K$  is a shape factor. Draxler and Hess (1997) allow  $K$  to vary between 1.0 and 2.0, although other texts allow maximum values greater than 2.0. The Cunningham slip correction is also included in the Stokes equation in the HYSPLIT model, but there is no need here to consider it further.

The Stokes equation is applicable only to the laminar region of the standard drag curve for spherical objects, in the vicinity of Reynolds number less than approximately 0.05 to 1 (Green and Lane 1964). This region corresponds to small particles, less than approximately 20 microns in diameter. For particles larger than this, the Stokes solution underestimates drag on the particle and consequently overestimates its TFV. Measurements have shown that volcanic ash particles vary widely in size, both above and below a diameter of 20 microns. The Stokes equation is therefore not entirely suitable for estimating the TFVs of volcanic ash particles. An alternative equation must be considered for the accurate prediction of TFVs of volcanic ash over the wide range of particle sizes that have been observed.

There are numerous equations available for computing the drag on spherical particles over a wider range of Reynolds numbers (and particle sizes) than predicted by the Stokes equation. However, while these account for particle density and size, they do not all include consideration of the particle's shape. The study of Chhabra et al. (1999) contained rigorous tests of several equations used to predict TFVs of particles based on size, density and shape. They recommended the use of the Ganser (1993) formulation. In addition, and relevant to the current work, the Ganser equation has been used in the prediction of the TFVs of volcanic ash particles in other models (for example, Scollo et al. 2008). Based on these points, the Ganser formulation (Equation 2) is selected for implementation into the version of the HYSPLIT model used in the current work concerned with motions of volcanic ash particles.

The Ganser equation defines drag coefficient,  $C_D$ , in terms of the Reynolds number and two shape factors.

$$C_D = \frac{24}{ReK_1} (1 + 0.1118(ReK_1K_2)^{0.6567}) + \frac{0.4305 K_2}{1 + \frac{2305}{ReK_1K_2}} \quad (2)$$

where  $Re$  is the Reynolds number (Equation 6) and  $K_1$  and  $K_2$  are shape factors (Equations 3 and 4, respectively) defined as functions of the particle's sphericity,  $\phi$ . Sphericity is defined by Wadell (1932) as the ratio of the surface area of a sphere with the same volume as the particle to the actual surface area of the particle.

$$K_1 = \frac{3}{1 + \frac{2}{\sqrt{\phi}}} \quad (3)$$

$$K_2 = 10^{1.8148 (-\log \phi)^{0.5743}} \quad (4)$$

Differences in TFVs predicted by the Stokes and Ganser equations are shown by Fig. 1. Very small deviations are evident for diameters less than 10 microns, while above this size the differences become very large. At approximately 57 microns, the differences reach 10 per cent, growing rapidly as the particle size increases to 20 per cent at 83 microns, and 50 per cent near 140 microns. As the Ganser equation approximates the standard drag curve at higher Reynolds Numbers, these percentage differences shown in Fig. 1 also represent errors in the TFVs predicted by the Stokes equation.

The Ganser equation is solved iteratively using Equations 5 and 6, the latter which defines the Reynolds number.

$$TFV = \sqrt{\frac{4 g d (\rho_p - \rho_{AIR})}{3 C_D \rho_{AIR}}} \quad (5)$$

$$Re = \frac{\rho_{AIR} TFV d}{\mu} \quad (6)$$

In practical terms, it may be useful to note another difference between the Stokes and Ganser equations. The dynamic shape factor  $K$  in Equation 1 has values greater than or equal to unity. In contrast, in Equations 3 and 4 sphericity is less than or equal to unity. In both cases, unity represents a perfectly spherical particle.

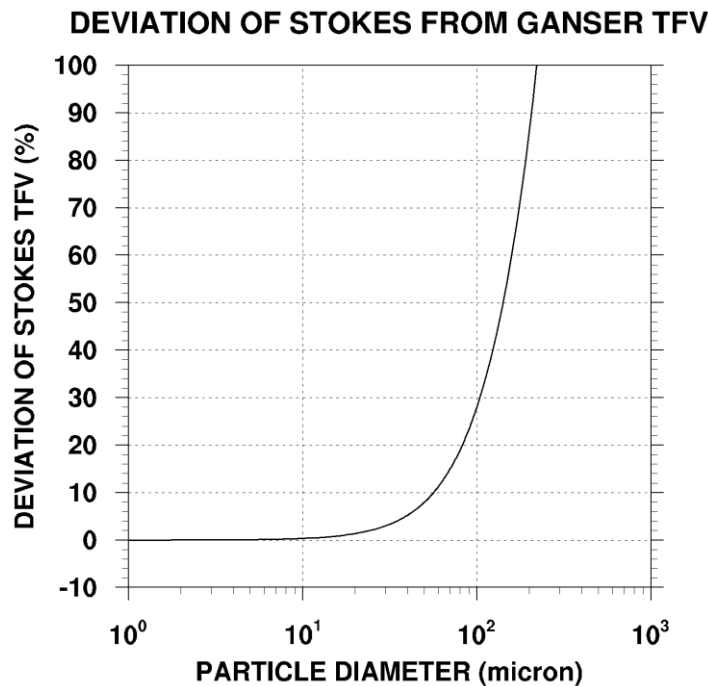


Fig. 1 Differences in TFV predicted by the Stokes and Ganser equations versus particle diameter.

### 3 PROPERTIES OF VOLCANIC ASH PARTICLES

To implement the change from modelling the dispersion of gas to that of solid particles, definitions of volcanic ash particle properties are required. These properties are density, shape, and size. These are important to define as accurately as possible because, along with the equation used, they affect the TFV of the ash particles, and therefore the time taken to fall to lower levels and eventually to the ground. Wind speeds and directions change with height in the atmosphere, with location, and also over time. The TFV of an ash particle therefore affects the height of the particle at any moment, and consequently the particular wind speed and direction experienced by, and responsible for the movement of, the particle. The initial height of the volcanic ash cloud is also an important factor affecting the time spent in the atmosphere, but this is not addressed in this report.

Although many observations of volcanic ash properties have been made and published, a challenge facing all parties concerned with the dispersion of volcanic ash is the fact that these properties are highly variable, making it very difficult to define these parameters for a particular eruption, particularly under the time constraints of operational forecasting. These properties vary between volcanoes, between eruptions (Martin et al. 2009), and even during a single eruption (Scollo et al. 2008).

#### 3.1 Density

The observed density of volcanic ash particles is highly variable. Values range from 245 to 3200 kg m<sup>-3</sup> (Bonadonna and Phillips 2003). Often, it is convenient or necessary to assume a single value of density. For example, 2300 kg m<sup>-3</sup> was used by Francis et al. (2012) and Devenish et al. (2012), while Heffter and Stunder (1993) and Draxler and Hess (1998) used a value of 2500 kg m<sup>-3</sup>, and Miffre et al. (2012) used 2600 kg m<sup>-3</sup>. In general agreement with these examples, the value used here in the HYSPLIT model is 2500 kg m<sup>-3</sup>.

#### 3.2 Shape

To use the TFV equation within the model it is necessary to represent the shape of the particle using a numerical value. A variety of parameters has been suggested. For consistency with the Ganser TFV formulation, the shape factor used here is sphericity. In common with many shape factors, a value of 1.0 represents a sphere, with smaller values representing departure from a perfect sphere. The assumption of spherical particles is not uncommon in other work concerned with volcanic ash properties, including dispersion modelling (Heffter and Stunder 1993, Devenish et al. 2012). For the initial experiment presented here (experiment number 2) concerned with a comparison between solid particles and gas, sphericity is allowed to remain at unity in order to allow a clear assessment of the impact of the main two modifications introduced to the model in the current work (the new TFV formulation and the change from gas to solid particles). In other experiments that follow (see Table 1), the sphericity is varied over a range of realistic values, based on Riley et al. (2003) and Alfano et al. (2011). It is not possible to reliably define a mean value of sphericity for volcanic ash particles because values vary depending on the particular sample of particles analysed. However, a value of approximately 0.8 is appropriate based on values presented by Riley et al. (2003) and Alfano et al. (2011).

### 3.3 Size

The diameters of volcanic ash particles range upward from approximately 0.1-0.3 micron (Witham et al. 2012). The variation in relative mass across the range of particle sizes leads to consideration of a particle size distribution (PSD) rather than particular particle sizes or range of particle sizes. The PSD adopted here for these initial experiments (Fig. 2) approximates that observed by Hobbs et al. (1991), and used previously in dispersion modelling by Heffter and Stunder (1993), Dacre et al. (2011) and Devenish et al (2012).

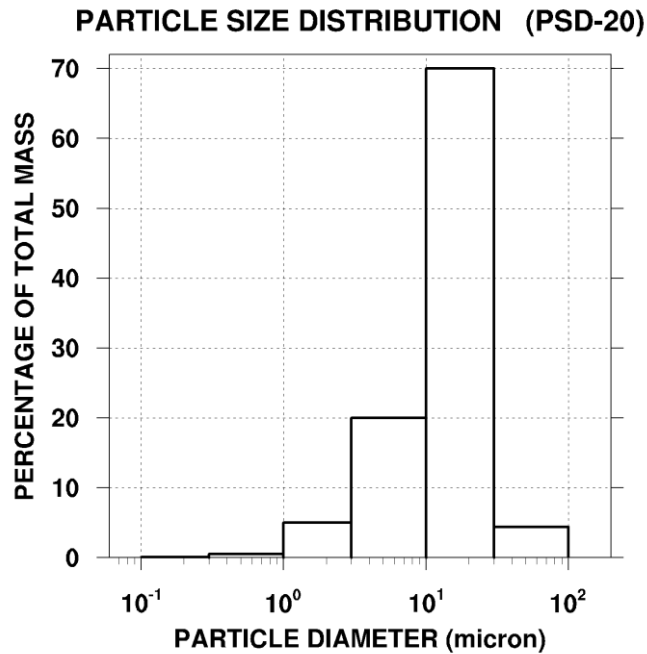


Fig. 2 Particle size distribution (particle diameter versus percentage of mass contained in each discrete particle size bin). With a peak percentage centred on 20 micron, this PSD is referred to as PSD-20.

MODEL EXPERIMENT	GAS/PSD	DENSITY (kg m <sup>-3</sup> )	SHAPE FACTOR (SPHERICITY)
1	GAS	----	----
2	PSD-20	2500	1.0
3	PSD-20	2500	0.8
4	PSD-20	2500	0.6
5	PSD-20	2500	0.4
6	PSD-20	2000	1.0
7	PSD-20	1500	1.0
8	PSD-20	1000	1.0
9	PSD-20	2000	0.8
10	PSD-20	1500	0.6
11	PSD-20	1000	0.4
12	PSD-6.5	2500	1.0
13	PSD-65	2500	1.0

Table 1 Physical properties of volcanic ash particles used in each model experiment.

## **4 MODEL SIMULATION RESULTS: GAS VERSUS SOLID PARTICLES**

### **4.1 Introduction**

The modifications to the model physics (Section 2) and the definition of particle properties (Section 3) described above are applied to a model simulation of the dispersion of a volcanic ash cloud. The case considered here is the recent eruption of Sangeang Api in Indonesia. This eruption began at 08 UTC on 30 May 2014 and continued for 1 hour. The eruption column reached a height of approximately 15 km. Flights were disrupted in the vicinity of Darwin, located more than 1000 km from Sangeang Api.

The aim here is to consider two main aspects of the performance of the model following the various modifications. First, the physical realism of the model results is assessed. Second, comparisons are made between the new system that simulates the dispersion of solid particles and the previous version that modelled dispersion of gas. Two model experiments were conducted, the first with a gas and the second with solid particles, as shown by experiment numbers 1 and 2 in Table 1. Data input to the model were identical, except that the PSD shown in Fig. 2 was used in the solid particle experiment, while in the other, a gas was released. The same model executable was used for both simulations. The total masses emitted in the volcanic column (a line source between the ground and 15 km) were identical between the two simulations. In each case, mass was released over a period of one hour from 08 to 09 UTC on 30 May 2014, producing a total of 1 arbitrary unit of mass. This allows for a clear comparison between the concentrations predicted by the respective model simulations.

### **4.2 18-hour model forecast of volcanic ash dispersion**

The prediction by the model of the position of gas in the 0-5000 metre layer after dispersion from Sangeang Api is shown in Fig. 3a, at 02 UTC 31 May 2014, 18 hours after the eruption began. Shown in Fig. 3b is the corresponding prediction using the modified model with solid particles. A box is used in both Figs 3 and 4 to identify the area being discussed. To the west and south of the volcano, and outside of the box, the gas and solid particle predictions are remarkably similar in both shape and areal extent. The main difference in this part of the volcanic cloud is the concentration, with the gas cloud containing higher concentrations, particularly to the southwest and west of the volcano. The concentrations in the gas cloud may be higher than those in the solid particle cloud because the solid particles are capable of falling to the ground, thereby lowering the concentration in the atmospheric layer up to 5000 metres above the surface.

A more striking difference between the gas and solid particle simulations is the presence of a very extensive cloud in Fig. 3b (identified by the box) extending for hundreds of kilometres to the southeast, towards Australia. This feature is totally absent in the gas simulation (Fig. 3a), even though the two simulations began with equal masses at the same location. The challenge is to explain the origin of this additional mass. If this feature were due to differences in winds and turbulence between the two simulations, then one would expect that the gas and solid particle clouds outside the box would not be so very similar. An alternative explanation must therefore be used to explain the additional mass.

Examination of the 5000-10000 metre layer (Fig. 4) at the same time as the clouds shown above (02 UTC) shows the presence of a solid particle cloud (Fig. 4b) located directly to the east and above that found within the 0-5000 metre layer (Fig. 3b). Although solid particles from the cloud

at 5000-10000 metres fell into the 0-5000 metre layer in the preceding hours, the west-northwesterly winds in the 5000-10000 metre layer moved this ash cloud away to the east of the ash cloud in the 0-5000 metre layer that, in comparison, was subject to relatively weak northerly and north-northwesterly winds. Although in separate simulations, it is interesting that a gas cloud is also present at 5000-10000 metres (Fig. 4a) at a similar location. The point to note here is that the gas cloud in the 5000-10000 metre layer did not produce a cloud in the 0-5000 metre layer below, while a cloud was produced in the lower layer by the simulation using solid particles. This occurred because the experiment using solid particles was able to simulate the descent of volcanic ash particles from the 5000-10000 metre layer into the 0-5000 metre layer below.

There are two differences between the solid particle and gas clouds in the 5000-10000 metre layer. First, the areal extent of the solid particle cloud is greater than that of the gas cloud due to the solid particles experiencing changes in wind with height as they fall through the layer. Second, the concentration of the solid particle cloud is lower than that of the gas cloud in this layer.

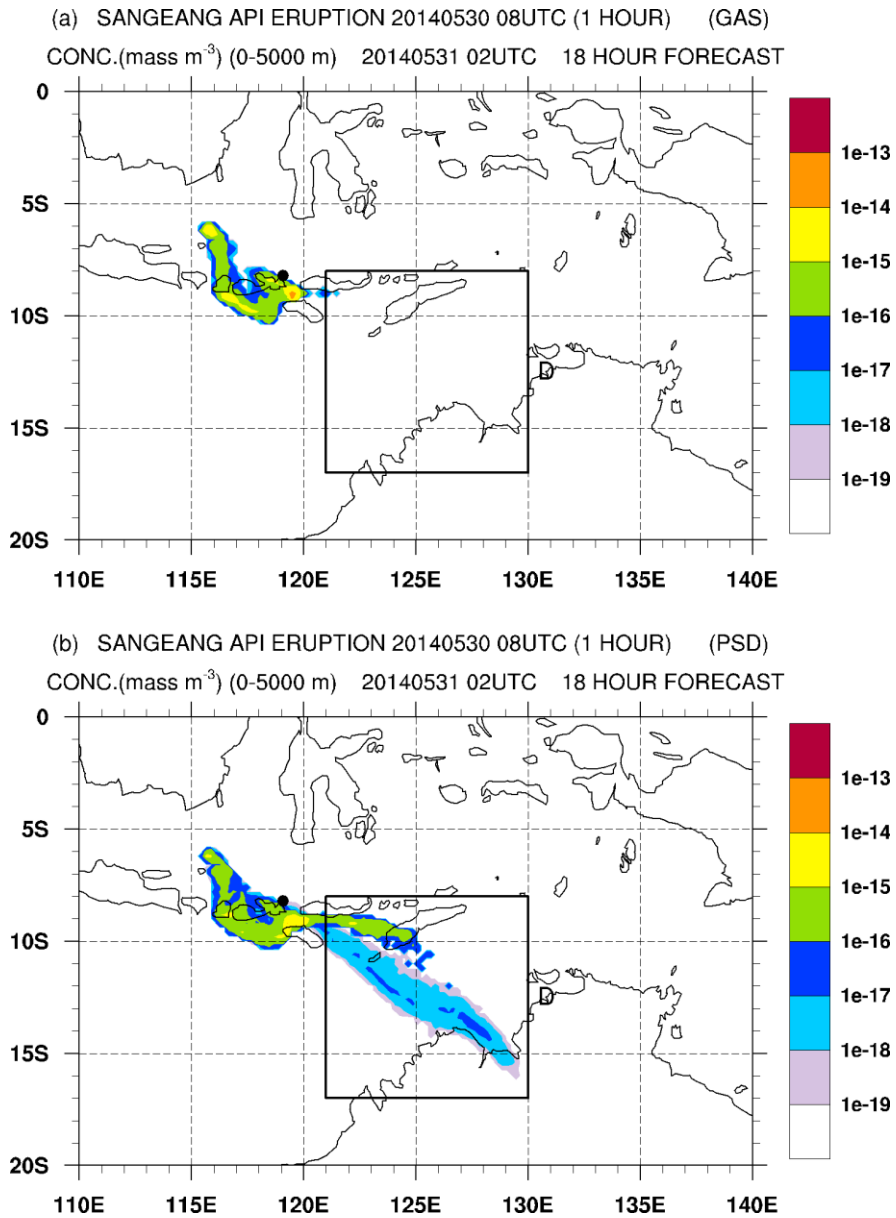


Fig. 3 Mean layer (0-5000 metres) concentration of volcanic cloud at 02 UTC 31 May 2014, 18 hours after the eruption began, for (a) gas simulation, (b) solid particle simulation. The location of the source volcano is shown by the black dot, and the location of Darwin is shown by "D".

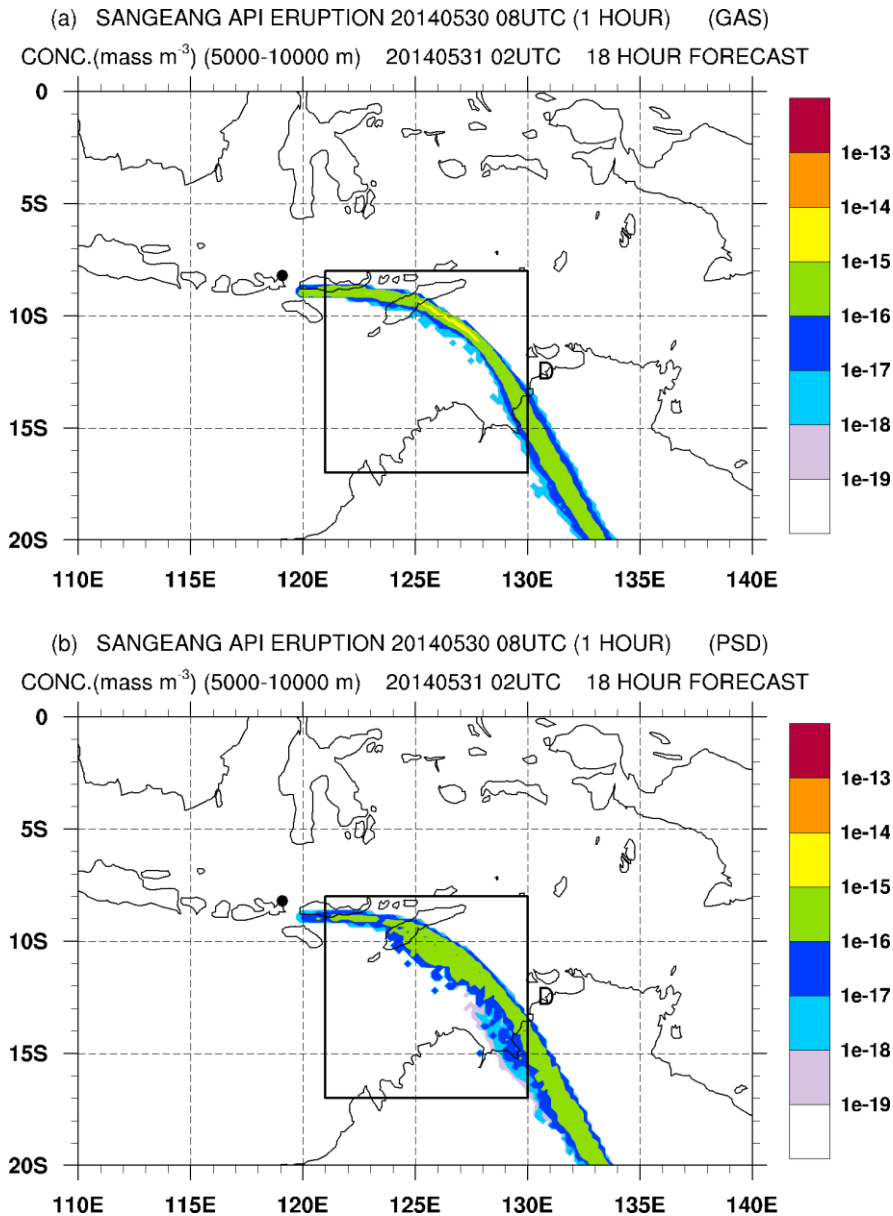


Fig. 4 Mean layer (5000-10000 metres) concentration of volcanic cloud at 02 UTC 31 May 2014, 18 hours after the eruption began, for (a) gas simulation, (b) solid particle simulation. The location of the source volcano is shown by the black dot, and the location of Darwin is shown by “D”.

### 4.3 24-hour model forecast of volcanic ash dispersion

Six hours later (08UTC), the gas simulation predicts that the volcanic cloud in the 0-5000 metre layer has remained in the vicinity of Indonesia (Fig. 5a). In contrast, the solid particle simulation for this time (Fig. 5b) shows that the ash cloud extends in two branches south-eastward to Australia, over the area close to and south of Darwin. The difference between these two predictions is very significant in terms of their ability to alert forecasters to the potential danger of volcanic ash in the vicinity of Darwin. At a higher level (5000-10000 metres), the respective locations of the gas and solid particle clouds are broadly similar (Figs 6a and 6b). However, the structures within the two clouds are different. The highest concentrations within the gas cloud (values above  $10^{-16}$ ) are found to extend from Indonesia to approximately 24°S over Australia. In contrast, concentrations above  $10^{-16}$  in the solid particle cloud are relatively smaller and fragmented, from Indonesia to approximately 19°S. However, south of this latitude, areas in the

solid particle cloud with concentrations above  $10^{-16}$  are larger than those in the corresponding gas cloud. Also significant is the large difference between the simulations in the spatial extent of the clouds close to Darwin. The simulation using solid particles has predicted the presence of an ash cloud to the south and west of Darwin, while the relatively narrow cloud produced by the gas-based simulation does not cover this area.

#### **4.4 Domain-integrated mass of volcanic ash**

To demonstrate a key difference in the functioning of the gas and solid particle simulations, a measure of the total mass versus height is considered at different times throughout the model simulation (Fig. 7). The mass here is represented by the areal integration of the mass load of solid particles within each layer. The initial mass total is 1.0, evenly distributed over three layers, each with a thickness of 5000 metres. Note that the data here represent total mass within a layer, which may not be representative of pollutant concentration at any one point within that layer.

From the end of the eruption at 09 UTC to 15 UTC on 30 May 2014, the mass decreases within the upper two layers but increases slightly in the lowest 0-5000 metre layer. From 15 UTC to 21 UTC, there is a further decrease in the 10000-15000 metre layer. However, in the 5000-10000 metre layer the mass is approximately balanced, as it receives particles falling from the 10000-15000 metre layer while at the same time losing particles to the 0-5000 metre layer. At 21 UTC, the mass in the lowest layer falls to its lowest point during the 24-hour period considered here.

Over the next 6 hours to 03 UTC on 31 May, the mass actually increases over this period in the lowest layer as particles continue to fall from above. Over this same period, the mass decreases in the upper two layers, and then again over the final 6 hours shown. Comparison between the mass present in the atmosphere at the first and final times shown here in Fig. 9 shows that the model atmosphere has lost mass to the surface. In contrast, the atmosphere in the gas-based simulation does not have the ability to lose mass to the surface due to gravity. Over the depth of the atmosphere, the solid particle simulation has lost approximately 15 per cent of its volcanic mass while the gas based simulation maintains 100 per cent of its volcanic pollutants.

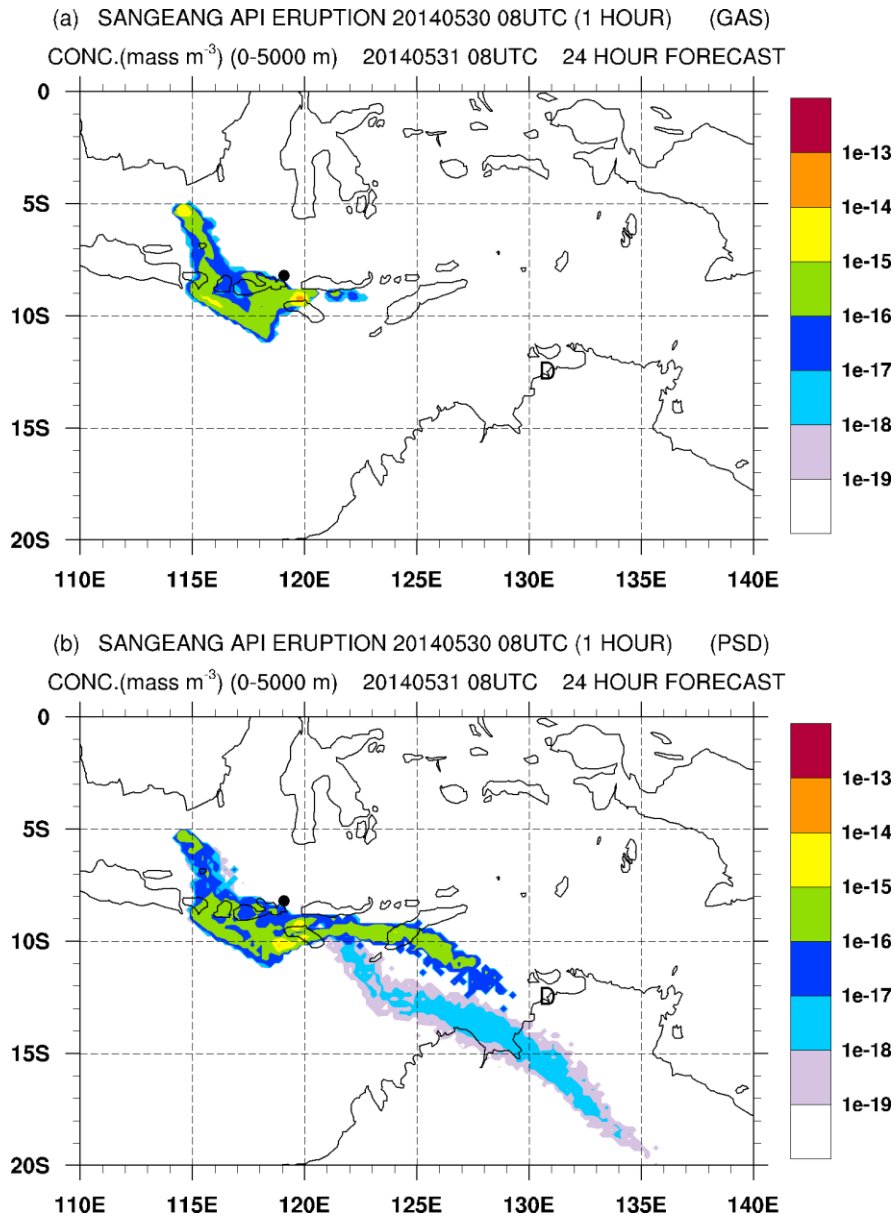


Fig. 5 Mean layer (0-5000 metres) concentration of volcanic cloud at 08 UTC 31 May 2014, 24 hours after the eruption began, for (a) gas simulation, (b) solid particle simulation. The location of the source volcano is shown by the black dot, and the location of Darwin is shown by "D".

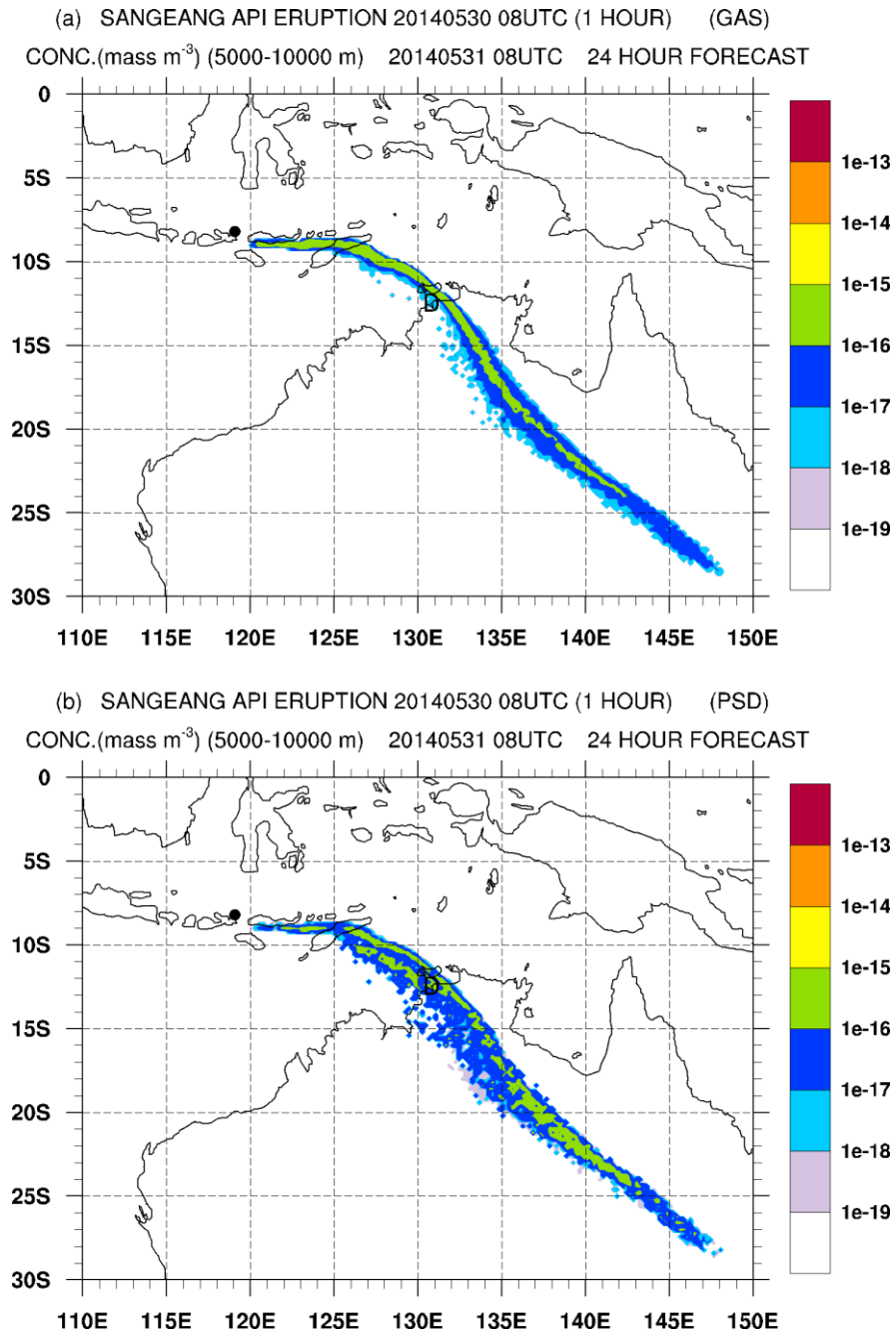


Fig. 6 Mean layer (5000-10000 metres) concentration of volcanic cloud at 08 UTC 31 May 2014, for (a) gas simulation, (b) solid particle simulation.

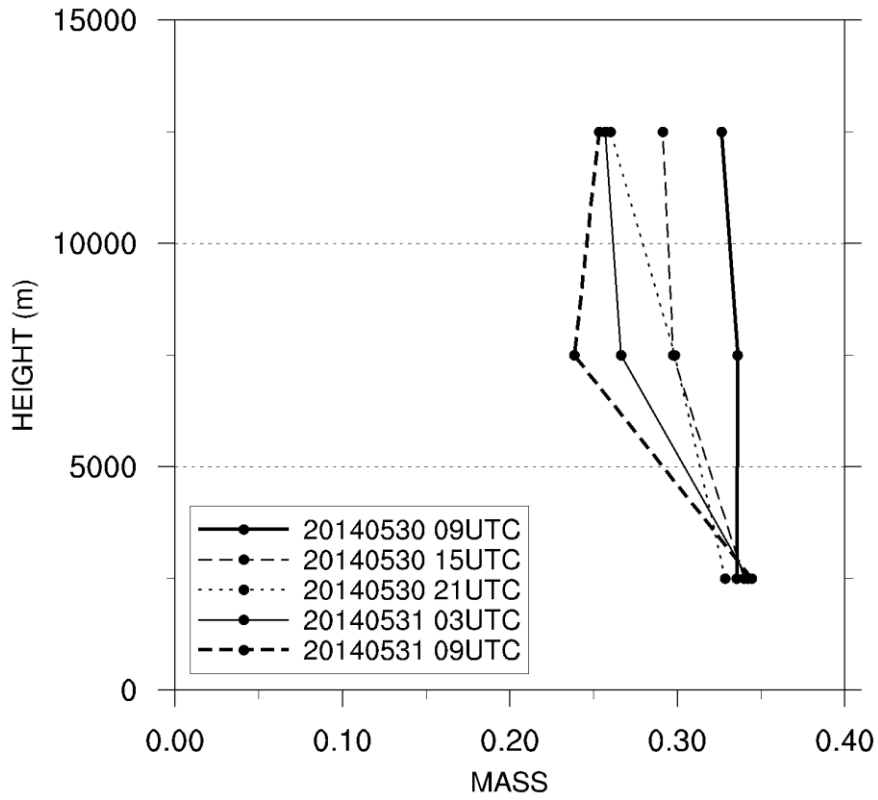


Fig. 7 Mass versus height display of layer- and areal-integrated mass load of solid particles during the 24 hour period following the end of the eruption, for the three layers 0-5000, 5000-10000 and 10000-15000 metres.

## 5 MODEL RESULTS: PHYSICAL PROPERTIES OF PARTICLES

### 5.1 Introduction

In addition to the two model experiments discussed above, eleven further experiments were conducted to test the sensitivity of the simulations to variations in the physical properties of the volcanic ash particles. The details of these experiments are listed in Table 1. The eleven experiments are divided into four groups, with the aim of comparing them with the initial solid particle experiment (experiment number 2 in Table 1).

In the first group (experiment numbers 3 to 5), the three experiments differed from experiment 2 in that the shape factors (sphericities) was reduced to values less than 1.0 to represent non-spherical particle shapes. In the second group, the shape factor remained equal to 1.0, while particle densities were reduced. In the third group, experiments 9 to 11, both the densities and shape factors were reduced.

In the fourth group, the PSD-20 shown in Fig. 2 was varied to produce two additional PSDs (Fig. 8), the first of which was used in experiment 12 and the second in experiment 13. The new PSDs were created by shifting half of the mass in the 10-30 micron bin to one of the neighbouring bins. That is, PSD-6.5 in Fig. 8a was created by removing half of the mass from the 10-30 micron bin (35 per cent of the total mass) and placing it in the 3-10 micron bin. Similarly, PSD-65 in Fig. 8b was created by shifting this 35 per cent of the total mass into the 30-100 micron bin. The dashed lines in Fig. 8 represent the percentages used in PSD-20 (Fig. 2), and are included here to identify differences between, and allow comparison of, the PSDs in Fig. 8 with that in Fig. 2.

### 5.2 Mass remaining in atmosphere

The amount of volcanic pollutant remaining in the atmosphere after a period of time, such as 24 hours, may be used to assess differences in results due to variations in the physical properties of particles used in each simulation. Figure 9 provides a comparison between all thirteen experiments in terms of the percentage of mass that was simulated to remain in the atmosphere after a period of 24 hours since the beginning of the eruption.

The amount of gas (experiment 1) remaining in the atmosphere after 24 hours was maintained throughout the simulation at 100 per cent. Experiment 2 predicted approximately 84 per cent after 24 hours, as 16 per cent of the total mass fell to the ground over the period. Experiments 2 to 5 used a particle density of  $2500 \text{ kg m}^{-3}$  and sphericities of 1.0, 0.8, 0.6, and 0.4, respectively. A lower sphericity represents a particle with a shape that is less spherical, meaning that the particle experiences increased drag, resulting in a lower TFV and an increased residence time in the atmosphere. Fig. 9 shows that the mass remaining in the atmosphere increased from approximately 84 to 89 per cent as the sphericities were reduced in these experiments. Considering that these sphericities cover a wide range of observed values for volcanic ash, the impact of sphericity on the remaining mass is not large. However, this may vary if alternative PSDs were considered, a point that will be discussed later.

In experiments 2 and 6 to 8, particle densities were reduced from  $2500 \text{ kg m}^{-3}$  to  $1000 \text{ kg m}^{-3}$ , while the sphericity was held constant with a value of 1.0. The reduced densities led to smaller

TFVs for the particles, which increased the time spent by each particle in the atmosphere. Consequently, the mass that remained in the atmosphere increased as the particle density was reduced. While the range of densities used here do fall within the range of observed densities for solid volcanic objects, it would be unusual to operate a dispersion model with a particle density as low as  $1000 \text{ kg m}^{-3}$ , but it was included here to demonstrate impacts from a range of particle densities.

In experiments 2 and 9 to 11, sphericity and density were both reduced. The amount of mass remaining in the atmosphere increased further, compared with experiments 3 to 8 discussed above, due to the combination of the reduced density and reduced sphericity (Fig. 9), as may be expected based on the trends found previously in experiments 3 to 5 and 6 to 8.

The use of PSD-6.5 in place of PSD-20 led to an increase of approximately 5 per cent in the amount of mass remaining in the atmosphere after a period of 24 hours (compare experiments 2 and 12 in Fig. 9). In PSD-6.5, a larger percentage of the total mass was represented by particles sized between 3 and 10 microns and less between 10 and 30 microns. The smaller particles fell more slowly, which resulted in more mass remaining in the atmosphere over this period.

When PSD-65 was used (experiment 13), the mass remaining in the atmosphere decreased dramatically compared with the mass remaining when PSD-20 was used (experiment 2). Although PSD-65 was created based on an apparently modest change to PSD-20, the impact on the total mass was the largest found in any of the experiments (Fig. 9). It is not possible to conclude which PSD is more suitable to use because PSDs differ between eruptions and evolve over time and distance from the source volcano as the volcanic ash cloud disperses. However, it is important to note the large impact that a PSD can have on a volcanic ash cloud, particularly when compared with the relatively smaller impacts found when particle densities and sphericities were varied over a wide range of values.

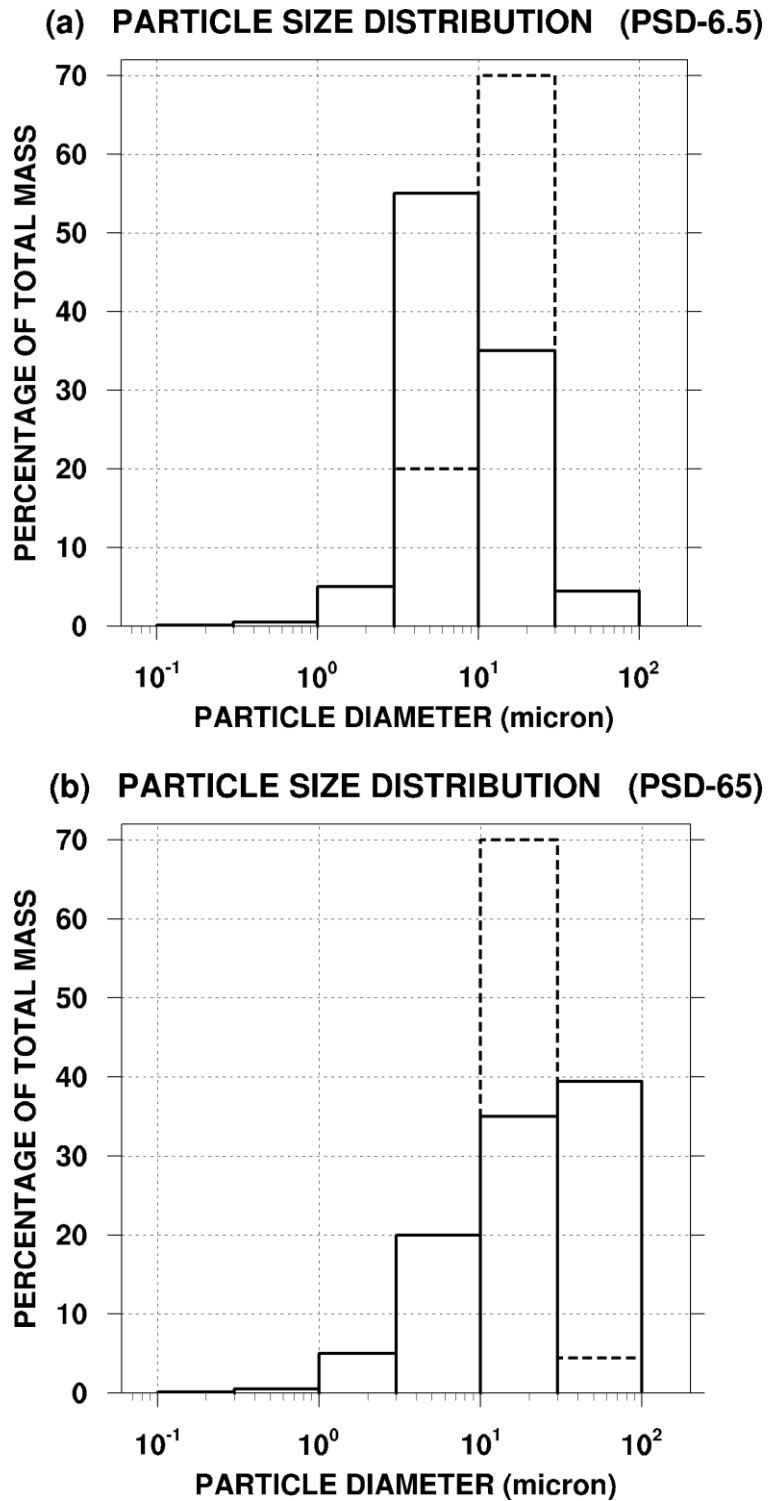


Fig. 8 Particle size distributions (particle diameter versus percentage of mass contained in each discrete particle size bin), with a peak percentage centred on (a) 6.5 micron (PSD-6.5) and (b) 65 micron (PSD-65). Dashed lines represent the original PSD shown by Fig. 2.

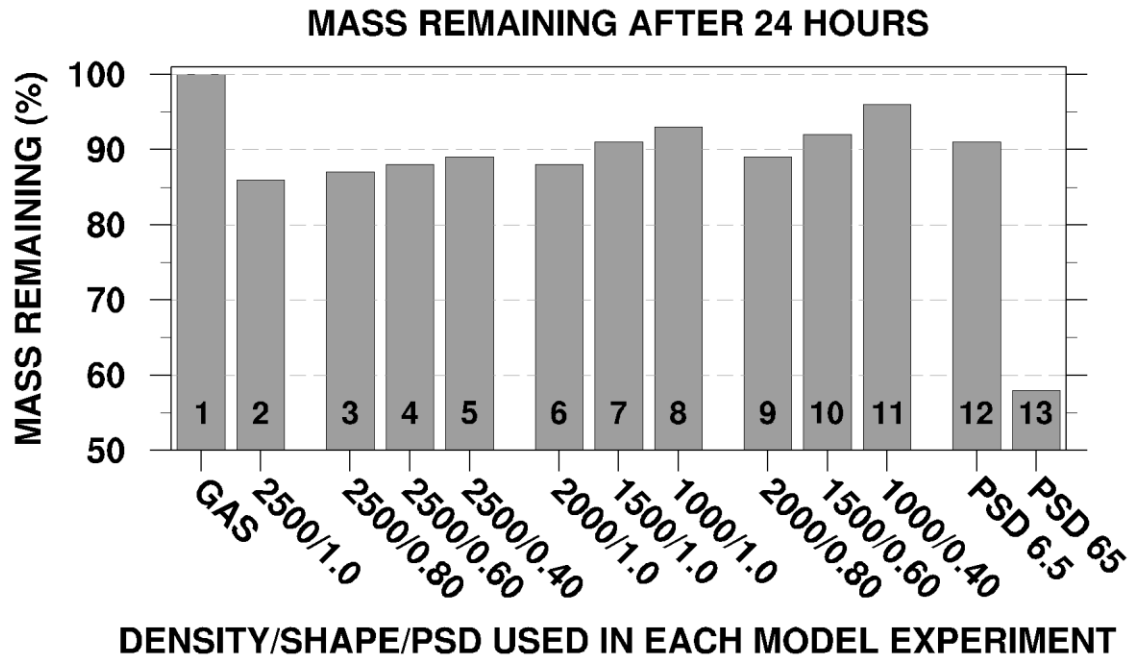


Fig. 9 Mass remaining in the atmosphere (percentage of total mass released) after a simulated period of 24 hours, for each of the thirteen experiments listed in Table 1.

### 5.3 Surface deposition of volcanic ash

The total deposition of solid particles on the Earth's surface predicted by four selected simulations (experiments 2, 11, 12 and 13) are shown in Fig. 10. The gas-based simulation did not, of course, produce any deposition and is not included. The depositions shown are time-integrated based on 1-hourly model outputs over a total period of 40 hours since the eruption began. As would be expected, the bulk of the surface deposition occurs close to the source volcano. The general pattern of deposition in these four simulations shows distribution of volcanic material along an axis to the northwest of the volcano, an area to the west, and a long arm to the southeast associated with the dispersion of the ash cloud towards Australia, as discussed previously (Figs 3 to 6).

The surface deposition that results from the initial solid particle simulation (experiment 2) is presented in Fig. 10a. The surface deposition produced from experiment 11 (Fig. 10b), in which the lowest values of sphericity (0.4) and density ( $1000 \text{ kg m}^{-3}$ ) were used, differs from experiment 2 mostly in the vicinity of the volcano, where there are lower values of deposition. It may be expected that lower values of these particle properties would result in lower values of deposition near the volcano because these particles would fall more slowly than those in experiment 2. A consequence of the longer residence time of the particles in experiment 11 is that they are subject to atmospheric motions for a longer period and therefore travel further from the source. This effect can be seen by the relatively longer surface deposition swath over Australia produced by experiment 11 (Fig. 10b) compared with that produced by experiment 2 (Fig. 10a).

The impact on surface deposition due to changes in the PSD can be seen by comparing Figs 10a (PSD-20), 10c (PSD-6.5) and 10d (PSD-65). There is very little difference between surface deposition patterns produced by simulations using PSD-20 and PSD-6.5. The use of very low values of density and sphericity (Fig. 10b) had a larger impact on surface deposition than did varying the PSD from PSD-20 to PSD-6.5. However, the use of PSD-65 had a larger impact. The

relatively larger fraction of mass in the 30-100 micron bin of PSD-65, the largest bin defined in all of the PSDs used here, might have been expected to result in a greater deposition of mass close to the volcano, but less difference between simulation results further away from the source. While there are differences close to the source, the clearest difference is found throughout the arm extending to the southeast, where a wide swath exists with surface depositions above  $10^{-15}$  (Fig. 10d). In comparison, the other three simulations shown here do not produce such high values of surface deposition as far as  $130^{\circ}\text{E}$  to  $135^{\circ}\text{E}$ . While the use of PSD-65 had a relatively very large impact on the mass remaining in the atmosphere, as shown by experiment 13 in Fig. 9, this PSD was not so extreme as to greatly affect the areal coverage of the surface deposition.

#### **5.4 Volcanic ash concentration in the 10000-15000 metre layer**

In Sections 5.2 and 5.3, the impacts of changes in the physical properties of volcanic ash particles were considered in terms of the mass remaining in the atmosphere and the mass deposited on the ground. In this section, the impact of these same changes on the concentration of volcanic ash in the 10000-15000 metre layer is considered. Concentrations of volcanic ash in this layer are shown by Figs 11a-d for the same four experiments (2, 11, 12 and 13) as considered in Figs 10a-d, but with the addition of experiment 1 in Fig. 11e.

All simulations have dispersed the pollutants over eastern Australia in clouds with similar shapes and areal extents. The concentrations of volcanic ash within each of the clouds define the difference between the results of each experiment. Every experiment shown in Fig. 11 has produced an area of high concentration ( $> 10^{-16}$ ) in the south-eastern part of the cloud, with relatively lower concentrations ( $10^{-17}$  to  $10^{-16}$ ) throughout the rest of the cloud.

The extent of the area in the northern-most swath of the cloud with concentrations above  $10^{-16}$  varies between all experiments. The gas experiment (Fig. 11e) produced the largest area of these high concentrations. In contrast, the initial solid particle simulation (Fig. 11a) predicted much lower concentrations in this layer at this location because volcanic ash particles were simulated to fall into lower layers, as discussed in Section 4. Differences between these two experiments have the potential to improve forecasting because the more physically realistic simulation using solid particles indicates that the area of ash over eastern Australia with concentrations above  $10^{-16}$  was less affected by volcanic ash than suggested by the gas-based simulation.

The experiment using very low values of density and sphericity (experiment 11) predicted higher concentrations of ash in the northern swath (Fig. 11b) than those predicted by experiment 2 (Fig. 11a). Although very low values of density and sphericity were used, the concentrations that resulted were lower than those produced by the gas simulation. This is an important point because even when very low values of density and sphericity were used (possibly even too low), the results differed from those produced from the experiment that simulated the dispersion of gas.

The use of PSD-6.5 (Fig. 11c) altered the results compared with experiment 2, but the impact was less than that found when very low values of density and sphericity were used. The smallest area of ash concentration above  $10^{-16}$  was produced when PSD-20 was used (Fig. 11d). This area is much smaller than found in the other experiments.

The experiments discussed here all use reasonable, but different, values of particle properties and PSDs, yet the results show that there is an impact on the predicted size of the area of highest concentration of ash. As particle properties and PSDs vary between eruptions, and varying values have the potential to affect forecasts of ash concentration, a single default set of particle properties cannot be relied upon to provide an accurate forecast. Reliable observations of

individual eruptions are required to provide information in real time that can be used to produce accurate simulations of the dispersion of volcanic ash. Ensemble techniques may also be developed to overcome uncertainties in particle properties and PSDs.

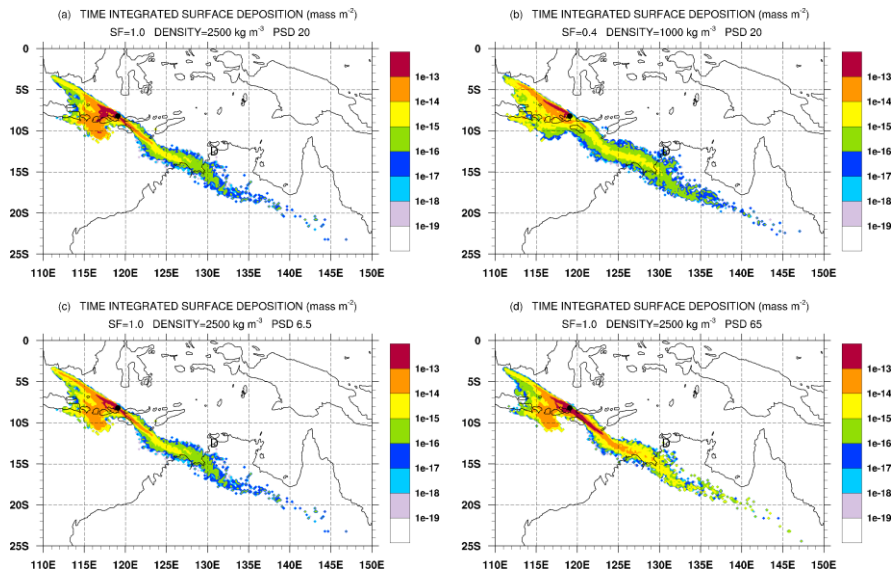


Fig. 10 Time-integrated (based on 1-hourly model output) surface deposition of volcanic ash (solid particles) over a 40-hour period since the beginning of the eruption. The location of the source volcano is shown by the black dot, and the location of Darwin is shown by “D”.

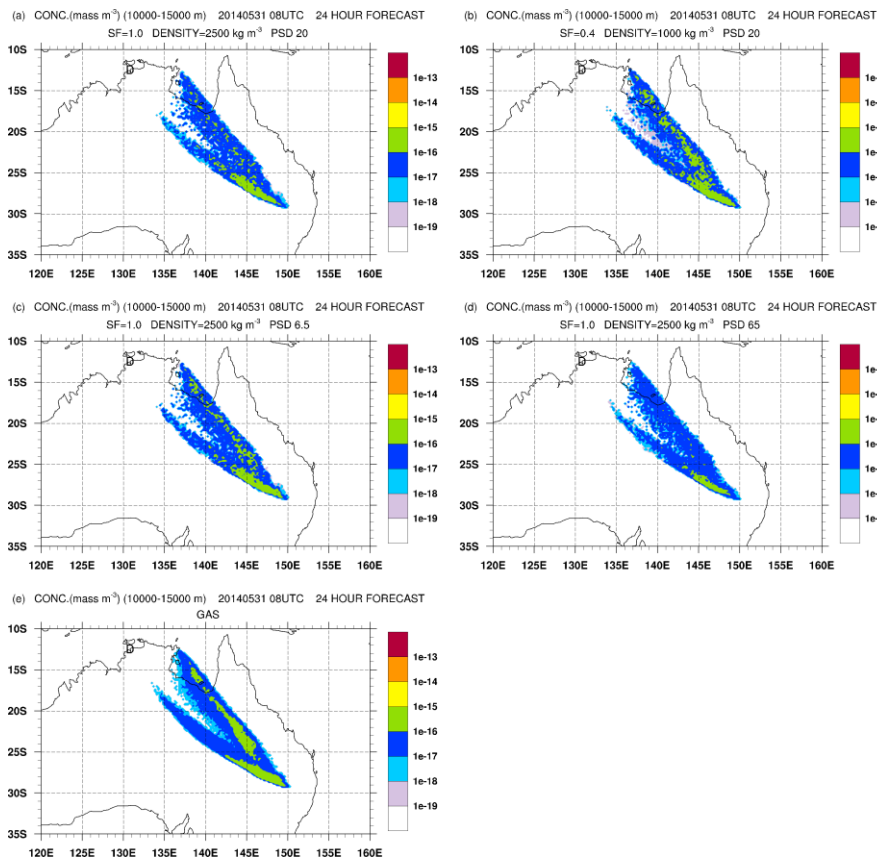


Fig. 11 Mean layer (10000-15000 metres) concentration of volcanic ash cloud at 08 UTC on 31 May 2014, 24 hours after the eruption began for experiments 2, 11, 12, 13, and 1.

## 6 SUMMARY

Solid ash particles injected into the atmosphere during volcanic eruptions have the potential to cause significant damage to aircraft engines, endangering lives and requiring expensive repairs. The aviation industry also suffers financially when flight operations are disrupted due to the presence of volcanic ash clouds in the vicinity of airports and flight paths. For all of these reasons it is important to improve the accuracy of observations and predictions of volcanic ash clouds.

In the past, the Australian VAAC has operated the HYSPLIT model using a gas to represent the cloud produced from an eruption. As gases and volcanic ash particles have very different properties and behave differently in the atmosphere, an essential requirement of the Improved Volcanic Ash Detection and Prediction Project is to replace simulations of gas dispersion with simulations of the dispersion of solid volcanic ash particles.

In this report, the first step was to assess the suitability of the formulation present within the HYSPLIT model for the prediction of TFVs of volcanic ash particles. The Stokes TFV equation, used in the HYSPLIT model, is applicable only to small particles less than approximately 20 microns in diameter. This limit is variable depending on one's own choice of error tolerance, as indicated by Fig. 1. A limit of around 5 to 10 microns may also be selected, but a value higher than 20 microns would result in increasingly inaccurate predictions by the Stokes equation. Observations of volcanic ash particles show that their sizes vary widely, both above and below this supposed limit of 20 microns. Therefore, it was decided to replace the Stokes TFV equation with a more suitable formulation. The Ganser equation was adopted as a replacement for the Stokes TFV equation, as it is applicable to the wide range of observed volcanic ash particle sizes.

Having selected an appropriate TFV formulation for use in the HYSPLIT model, the next step was to define appropriate values of density, shape and size to represent the physical properties of the population of volcanic ash particles. All three of these factors vary widely, between and even during eruptions, making it difficult to define them accurately. Single values for each factor were adopted based on published observations and values used in other modern dispersion models. The value adopted for particle density is  $2500 \text{ kg m}^{-3}$ , while a value of 0.8 is proposed to represent sphericity in future modelling.

Two model experiments were conducted based on the dispersion of the volcanic ash cloud from the recent Sangeang Api eruption. The first involved the dispersion of a gas, consistent with the past use of the HYSPLIT model at the VAAC. The second experiment involved solid volcanic ash particles. The impact of the use of solid volcanic ash particles in the model relative to that of a gas was assessed. The physical realism of the simulation following the modifications to the TFV formulation and the introduction of solid particles was also examined.

Results from the model experiment using the modified TFV formulation and solid particles confirmed that the movements of volcanic ash particles were simulated with a level of physical realism not achieved by the gas-based experiment. Volcanic ash simulated to fall from one model layer reduced the concentration, while increasing the concentration in lower layers, as required. Depending on the range of particle sizes involved, in combination with ambient winds and turbulence, the evolution of volcanic ash concentrations were simulated much more realistically than would be possible using gas as the volcanic emission. This is because the simulated gas molecules, while subject to ambient winds and turbulence, were not subject to the variety of TFVs predicted for the variety of particle sizes. As the solid particles moved to different heights in the model atmosphere, they were subject to different ambient wind speeds and directions, which then produced a result quite different from the gas-based simulation.

Examples were shown, such as in Fig. 4, where the gas-based model experiment produced concentrations of volcanic material within one atmospheric layer that were somewhat comparable with results from the solid particle experiment. However, in the model layer below (Fig. 3), the gas simulation contained much less material than found in the result from the solid particle experiment, where volcanic ash had been simulated to fall from the layer above. While this may appear to be a simple result due to the comparison between simulations of dispersion of gas and solid particles, results presented showed that the concentrations do not differ in a simple way. For example, in Fig. 6, the volcanic cloud produced by the two simulations may seem to be generally similar. However, the locations of the highest concentrations, which incidentally may be indicative of concentrations that are highly relevant in the assessment of hazards to aircraft, were found at very different locations depending on the use of gas or solid particles in the simulation.

Another interesting point, and an important result here, is that the experiment simulating the behaviour of solid volcanic ash particles not only affected concentrations at each layer in the atmosphere, but also had an impact on the areal extent of the hazardous cloud (Figs 4 and 6). This means that concentrations, locations within atmosphere layers, and the areal extent of volcanic ash clouds are all affected by the use of solid particles in place of a gas in model simulations.

Changes over time in the total mass of solid volcanic material within each 5000-metre layer were assessed by integrating over the entire horizontal model domain. In considering the 24-hour period following the end of the eruption, mass was gradually lost from all layers (Fig. 7). An interesting result is that the loss of mass was not consistent, and could even be reversed for a short period of time due to input from the layer above. Overall, the simulation using solid volcanic ash particles lost 14 per cent of its total mass by the end of this 24-hour period, which is a realistic result. In contrast, the gas-based experiment maintained its total mass at 100 per cent.

The model prediction using solid particles allowed for a physically-realistic simulation of the fall of volcanic ash to lower levels in the atmosphere. This allowed a different evolution of the distribution of solid volcanic particles in the vertical dimension. Solid particles were subject to wind speeds, directions and turbulence at heights and times that were all different from the corresponding ambient conditions imposed on the molecules present in the gas-based simulation. These differences led to different outcomes in concentrations of volcanic material within volcanic clouds. In addition to concentration, the areal extent of the volcanic cloud hazard was impacted. At some locations, the solid particle simulation produced ash clouds which were absent in the gas simulation.

Experiments used to evaluate the sensitivity of the model results to variations in particle density, sphericity and PSD showed that these parameters all have an impact. One aspect of this impact is well summarised by the percentage of the total mass remaining in the model atmosphere of each experiment after a period of 24 hours of simulation. Although the shape factor (sphericity) did not have a very large impact, there was some impact and therefore it would be sensible to represent the volcanic ash particles with improved realism, by adopting a value of sphericity that is less than unity, meaning non-spherical, in future model experiments. Although density and sphericity are different parameters with incompatible units, and cannot be strictly compared, variations in density over a realistic range appear to have a larger impact on the mass remaining in the atmosphere than do variations in sphericity over a realistic range of values.

While density and sphericity were varied over a wide range of values appropriate to volcanic ash particles, and their impacts were not negligible, these impacts were smaller than those found when relatively small changes were made to the PSD. It is relatively straight-forward to adopt

appropriate values of particle sphericity and density because ranges of values of these parameters are fairly well known. It is much more difficult to make a conclusion regarding the PSD because there is relatively less information available regarding PSDs, particularly airborne observations of PSDs in volcanic ash clouds. This is a challenge because the experiments conducted here indicate that the particular nature of the PSD has the potential to have a large impact on the model results.

The modified model and the introduction of solid particles has allowed for a physically-realistic simulation of the evolution of the distribution of volcanic ash. Improving the realism of the representation of physical processes in a numerical model is a robust method to improve the accuracy of predictions.

## 7 RECOMMENDATIONS

- It is recommended that the Ganser terminal fall velocity equation be implemented in the operational version of the HYSPLIT model, as it is more appropriate for the prediction of terminal fall velocities of volcanic ash particles than the Stokes equation.
- It is recommended that the more physically realistic model configuration with a particle size distribution and improved particle fall speed should replace the current dispersion model runs that assume a gas.
- It is recommended that the model configuration established in this report be used as the basis for the development of an ensemble system for the prediction of volcanic ash cloud dispersion.
- In future, other processes in the dispersion model that affect the fallout of solid volcanic ash particles should be investigated and considered carefully, such as wet deposition, aggregation, convective motions, and the representation of turbulent mixing, as they all have the potential to impact the predicted concentrations and areal extents of volcanic clouds.
- It may be beneficial in future to review and test the choice of model level heights to find a set of levels that best represents the needs of forecasters when relying on numerical model guidance of volcanic ash at specific flight levels.
- Numerical model guidance accuracy may benefit in future from the possible coupling of a dispersion model with an eruption column plume model. In the past, these different types of models have been operated independently. Problems and impacts of coupling these different types of systems are unknown, but are likely to be quite complicated, and would need to be planned and investigated carefully.

## 8 REFERENCES

- Alfano, F., C. Bonadonna, P. Delmelle, and L. Costantini, 2011: Journal of Volcanology and Geothermal Research, 208, 86-98.
- Bonadonna, C. and J.C. Phillips, 2003: Sedimentation from strong volcanic plumes. Journal of Geophysical Research, 108, B7.
- Chhabra, R.P., L. Agarwal, and N.K. Sinha, 1999: Drag on non-spherical particles: an evaluation of available methods. Powder Technology, 101, 288-295.
- H.F. Dacre, A.L.M. Grant, R.J. Hogan, S E. Belcher, D.J. Thomson, B.J. Devenish, F. Marengo, M.C. Hort, J.M. Haywood, A. Ansmann, I. Mattis, and L. Clarisse, 2011: Evaluating the structure and magnitude of the ash plume during the initial phase of the 2010 Eyjafjallajökull eruption using lidar observations and NAME simulations. Journal of Geophysical Research, 116, D00U03.
- Devenish, B.J., P.N. Francis, B.T. Johnson, R.S.J. Sparks, and D.J. Thomson, 2012: Sensitivity analysis of dispersion modeling of volcanic ash from Eyjafjallajökull in May 2010. Journal of Geophysical Research, 117, D00U21.
- Draxler, R.R., and G.D. Hess, 1997: Description of the HYSPLIT\_4 modeling system. NOAA Tech. Memo. ERL ARL-224, 24 pp.[NTIS PB98-116593.]
- Draxler, R.R., and G.D. Hess, 1998: An overview of the HYSPLIT\_4 modeling system for trajectories, dispersion, and deposition. Aust. Meteor. Mag., 47, 295-308.
- Francis, P.N., M.C. Cooke, and R.W. Saunders, 2012: Retrieval of physical properties of volcanic ash using Meteosat: A case study from the 2010 Eyjafjallajökull eruption. Journal of Geophysical Research, 117, D00U09.
- Ganser, G.H., 1993: A rational approach to drag prediction of spherical and nonspherical particles. Powder Technology, 77, 143-152.
- Green, H.L. and W.R. Lane, 1964: Particulate clouds, dusts, smokes and mists. Spon Ltd. London, pp. xvii, 471.
- Heffter, J.L. and B.J.B. Stunder, 1993: Volcanic Ash Forecast Transport And Dispersion (VAFTAD) Model, Weather and Forecasting, 8, 533-541.
- Hobbs, P.V., L.F. Radke, J.H. Lyons, R.J. Ferek, D.J. Coffman, and T.J. Casadevall, 1991: Airborne measurements of particle and gas emissions from the 1990 volcanic eruptions of Mount Redoubt. Journal of Geophysical Research, 96, D10, 18735-18752.
- Martin, R.S., T.A. Mather, D.M. Pyle, M. Power, V.I. Tasnev, C. Oppenheimer, A.G. Allen, C.J. Horwell, and E.P.W. Ward, 2009: Size distributions of fine silicate and other particles in Masaya's volcanic plume. Journal of Geophysical Research, 114, D09217.
- Miffre, A., G. David, B. Thomas, P. Rairoux, A.M. Fjaeraa, N.I. Kristiansen, and A. Stohl, 2012: Volcanic aerosol optical properties and phase partitioning behavior after long-range advection characterized by UV-Lidar measurements. Atmospheric Environment, 48, 76-84.

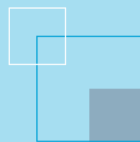
Riley, C.M., W.I. Rose, and G.J.S. Bluth, 2003: Quantitative shape measurements of distal volcanic ash. *Journal of Geophysical Research*, 108, B10.

Scollo, S., A. Folch, and A. Costa, 2008. A parametric and comparative study of different tephra fallout models. *Journal of Volcanology and Geothermal Research*, 176, 199–211.

Wadell, H. (1932) Volume, Shape, and Roundness of Rock Particles, *The Journal of Geology*, 40, 443-451.

Witham, C., H. Webster, M. Hort, A. Jones, and D. Thomson, 2012: Modelling concentrations of volcanic ash encountered by aircraft in past eruptions. *Atmospheric Environment*, 48, 219-229.





The Centre for Australian Weather and Climate Research is a partnership between CSIRO and the Bureau of Meteorology.